Polygonal chains cannot lock in 4D [☆]

Roxana Cocan, Joseph O'Rourke [*]

Department of Computer Science, Smith College, Northampton, MA 01063, USA

Communicated by Godfried Toussaint; received 4 November 1999; accepted 26 February 2001

Abstract

We prove that, in all dimensions $d \geqslant 4$, every simple open polygonal chain and every tree may be straightened, and every simple closed polygonal chain may be convexified. These reconfigurations can be achieved by algorithms that use polynomial time in the number of vertices, and result in a polynomial number of "moves". These results contrast to those known for $d = 2$, where trees can "lock", and for $d = 3$, where open and closed chains can lock. © 2001 Elsevier Science B.V. All rights reserved.

Keywords: Polygonal chain; Bar framework; Knots; Locked chains

1. Introduction

1.1. Summary

A *polygonal chain* $P = (v_0, v_1, \ldots, v_n)$ is a sequence of consecutively joined segments $s_i = v_i v_{i+1}$ of fixed lengths $\ell_i = |s_i|$, embedded in space. A chain is *closed* if the line segments are joined in cyclic fashion, i.e., if $v_n = v_0$; otherwise, it is *open*. A *polygonal tree* is a collection of segments joined into a tree structure. A chain or tree is *simple* if only adjacent edges intersect, and only then at the endpoint they share. We study reconfigurations of simple polygonal chains and trees, continuous motions that preserve the lengths of all edges while maintaining simplicity. One basic goal is to determine if an open chain can be *straightened*—stretched out in a straight line, and whether a closed chain can be *convexified*—reconfigured to a planar convex polygon. For trees, straightening permits noncrossing violations of simplicity to allow the segments to align along a common straight line. If an open chain or tree cannot be straightened, or a closed chain convexified, it is called *locked*. This terminology is borrowed from [3,4]. [1]

---

[*] Corresponding author.
E-mail addresses: rcocan@cs.smith.edu (R. Cocan), orourke@cs.smith.edu (J. O'Rourke).

[1] Straightening for trees is never defined in [4]. Instead they rely on mutually unreachable simple configurations.

Table 1

Dimension	Chains	Trees
2	Cannot lock	Lockable
3	Lockable	Lockable
$d \geqslant 4$	*Cannot lock*	*Cannot lock*

Most of the work in this area was fueled by the longstanding open problem of determining whether every open (or closed) chain in 2D can be straightened (or convexified). This was recently settled [8] in the affirmative: 2D chains cannot lock. In contrast it was earlier established that trees in 2D [4], and both open and closed chains in 3D [3,5] can lock. In this paper we prove that, for all dimensions $d \geqslant 4$, neither chains (open or closed) nor trees can lock. We partition our results into four main theorems:

Theorem 1. *Every simple open chain in 4D may be straightened, by an algorithm that runs in $O(n^2)$ time and $O(n)$ space, and which accomplishes the straightening in $O(n)$ moves.*

Here "move" is used in the sense defined in [3]. [2] Essentially each move is a simple monotonic rotation of a few joints. We have implemented this algorithm for the case when the vertices are in general position, when it is straightforward.

Nearly the same algorithm proves the same result for trees, within the same bounds:

Theorem 2. *Every simple tree in 4D may be straightened, by an algorithm that runs in $O(n^2)$ time and $O(n)$ space, and which accomplishes the straightening in $O(n)$ moves.*

Closed chains require more effort:

Theorem 3. *Every simple closed chain in 4D may be convexified, by an algorithm that runs in $O(n^6 \log n)$ time, and which accomplishes the straightening in $O(n^6)$ moves.*

All these results easily extend to higher dimensions.

Theorem 4. *Theorems 1–3 hold for all dimensions $d \geqslant 4$, i.e., neither polygonal chains nor trees can lock in dimensions greater than three.*

We summarize our results in the context of earlier work in Table 1.

1.2. Background

Before commencing with our technical arguments, we start with some background, with the intent of providing intuition to support our results.

---

[2] "During each move, a (small) constant number of individual joint moves occur, where for each a vertex v_{i+1} rotates monotonically about an axis through joint v_i, with the axis of rotation fixed in a reference frame attached to some edges."
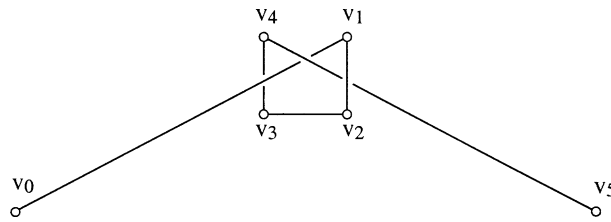
Fig. 1. The "knitting needles" example, based on Fig. 1 in [3] (by permission).

No knots in 4D. In [3,5], the same example of a locked open chain in 3D is provided. The version in the latter paper is shown in Fig. 1.

One proof (used in [3]) that this chain K is locked depends on closing the chain by connecting v_0 to v_5 to form K', and then arguing that K can be straightened iff the corresponding trefoil knot K' can be unknotted, which of course it cannot. Thus there is a close connection in 3D between unknotted, locked chains and knots. However, the following theorem is well known:

Theorem 5. *No 1D closed, tame,* [3] *non-self-intersecting curve C is knotted in $\mathbb{R}^4$.*

See, e.g., [1, pp. 270–271] for an informal proof. Because proofs of this theorem employ topological deformations, it seems they are not easily modified to help settle our questions about chains in 4D. The rigidity of the links prevents any easy translation of the knot proof technique to polygonal chains. However, it does suggest that it would be difficult to construct a locked chain by extending the methods used in 3D.

No cages in 4D. A second consideration lends support to the intuition behind our main claim. This is the inability to confine one segment in a "cage" composed of other segments in 4D. Consider segment $s_0 = v_0v_1$ in Fig. 1. It is surrounded by other segments in the sense that it cannot be rotated freely about one endpoint (say v_0) without colliding with the other segments. Let S be the 2-sphere in $\mathbb{R}^3$ of radius ℓ_0 centered at v_0. Each point on S is a possible location for v_1. Segment s_0 is confined in the sense that there are points of S that cannot be reached from s_0's initial position without collision with the other segments. This can be seen by centrally projecting the segments from v_0 onto S, producing an "obstruction diagram". It should be clear that v_1 is confined to a cell of this diagram. Although this by no means implies that the chain in Fig. 1 is locked, it is at least part of the reason that the chain might be locked.

We now argue informally that such confinement is not possible in 4D. Again let $s_0 = v_0v_1$ be fixed at v_0, and let S be the 3-sphere in $\mathbb{R}^4$ of radius ℓ_0 centered on v_0 that represents the possible locations for v_1. Again we project the other segments onto S producing an obstruction diagram. As in the lower dimensional case, this diagram is composed of 1D curves, being the projection of 1D segments. But in the 3-sphere S, v_1 has three degrees of freedom, and cannot be confined by a (finite) set of 1D curves. Our next task is to make this intuitive argument more precise.

---

[3] A curve is *tame* if it is topologically equivalent to a polygonal curve [9, p. 5]. Any curve that is continuously differentiable, i.e., in class C^1, is tame.

2. Straightening open chains in 4D

Let P be a simple, open polygonal chain in 4D with $n \geqslant 2$ vertices. Each vertex v_i is also called a *joint* of the chain. The segment $s_i = v_i v_{i+1}$ we sometimes call a *link* of the chain. We say a joint v_i is *straightened* if (v_{i-1}, v_i, v_{i+1}) are collinear and form a simple chain; in this case, the angle at v_i is π.

We prove Theorem 1 by straightening the first joint v_1, "freezing" it, and repeating the process until the entire chain has been straightened. This is a procedure which, of course, could not be carried out in 3D. But there is much more room for maneuvering in 4D. We have two different algorithms for accomplishing this task. The first (Algorithm 1a) is easier to understand, but only establishes a bound of $O(n^4)$ on the number of moves, and requires $O(n^4 \log n)$ time. The second (Algorithm 1b) is a bit more intricate but achieves $O(n)$ moves in $O(n^2)$ time. Both follow the rough outline just sketched. We provide full details for Algorithm 1a, but only sketch Algorithm 1b.

Define the *goal position* v_g for v_0 (and $s_g = v_g v_1$ the goal position for s_0) as the unique position that represents straightening of joint v_1. Call the goal position *intersected* if $s_g \cap s_i \neq \emptyset$ for some $i > 2$; and otherwise call it *free*.

2.1. Algorithm 1a

A high-level view of the algorithm is as follows.

Algorithm 1a. Open chains
repeat until chain straightened do
    1. if s_g is *free* then
        Construct obstruction diagram $Ob(v_0)$ on 3-sphere.
        Apply motion planning to move v_0 to v_g.
    2. else s_g is *intersected*
        Construct obstruction diagram $Ob(v_1)$ on 2-sphere.
        Move v_1 so that the goal position is not intersected.

2.1.1. Step 1: s_g is free
Our argument depends on some basic intersection facts, which we formulate in $\mathbb{R}^d$ in a series of lemmas before specializing to the $d = 3$ and $d = 4$ cases we need.

Geometric intersections in $\mathbb{R}^d$. Let the coordinates of $\mathbb{R}^d$ be $x_1, x_2, \ldots, x_d$. A *k-flat* is the translate of a subspace spanned by k linearly independent vectors. Flats for $k = 0, 1, 2$ are also called points, lines and planes. A k-sphere is the set of points in a $(k + 1)$-flat at a fixed radius from a point (its *center*) in that flat. A 0-sphere is a set of two points, a circle is a 1-sphere, and the surface of a ball in $\mathbb{R}^3$ is a 2-sphere. When emphasizing the topology of a k-sphere, we will use the symbol $\mathbb{S}^k$.

Lemma 1. *The intersection of a 2-flat H (i.e., a plane) with a $(d - 1)$-sphere S in $\mathbb{R}^d$ is a circle, a point or empty.*

Proof. Translate and rotate the sphere and plane so that the sphere is centered on the origin, and the plane is parallel to the $x_1 x_2$-plane. The equations of the sphere S and the plane H are then:

$$S: \quad x_1^2 + x_2^2 + \cdots + x_d^2 = r^2, \tag{1}$$

$$H: \quad x_3 = a_3, \quad x_4 = a_4, \quad \ldots, \quad x_d = a_d, \tag{2}$$

where the a_i are constants. Let $A^2 = \sum_{i=3}^{d} a_i^2$. Then

$$S \cap H: \quad x_1^2 + x_2^2 + A^2 = r^2, \tag{3}$$

$$x_1^2 + x_2^2 = r^2 - A^2. \tag{4}$$

If $r^2 < A^2$, the intersection is empty. If $r^2 = A^2$, the intersection is the point $(0, 0, a_3, \ldots, a_d)$. If $r^2 > A^2$, the intersection is a circle in H with radius $\sqrt{r^2 - A^2}$ and center $(0, 0, a_3, \ldots, a_d)$. $\square$

Lemma 2. *The intersection of a (1D) line, ray or segment with a $(d-1)$-sphere S in $\mathbb{R}^d$ is at most two points, i.e., it either contains one or two points or is the empty set.*

Proof. Let $s = ab$ be a segment, and let the sphere center be c. Let H be the 2D plane determined by the three points a, b, c, i.e., H is the affine span of $\{a, b, c\}$. Because $s \subset H$, we must have $s = s \cap H$. So

$$s \cap S = (s \cap H) \cap S \tag{5}$$

$$= s \cap (H \cap S). \tag{6}$$

By Lemma 1, $H \cap S$ is a circle, and the claim for segments follows because a segment intersects a circle in at most two points. Rays and lines yield the same result by selecting a and b sufficiently large. $\square$

Let a, b and c be three distinct points in $\mathbb{R}^d$, such that c does not lie on the segment ab. Call the set of points that lie on rays that start at c and pass through a point of ab a *triangle cone* $\Delta_c(a, b)$. If (a, b, c) are collinear, the triangle cone degenerates to a ray.

Lemma 3. *The intersection of a triangle cone $\Delta_c(a, b)$ with a $(d-1)$-sphere S in $\mathbb{R}^d$ consists of at most two connected components—and, if c is the center of S, of at most one component—each of which is a circular arc or a point.*

Proof. Let $\Delta = \Delta_c(a, b)$, and let H be the 2D plane containing Δ. Because $\Delta \subset H$, $\Delta = \Delta \cap H$. So $\Delta \cap S = \Delta \cap (H \cap S)$. By Lemma 1, $H \cap S$ is a circle C in the plane containing Δ. So the problem reduces to the intersection of a triangle cone with a circle. As illustrated in Fig. 2(a), this intersection is at most one arc if the cone's apex c is at the center of the C (Δ_1 in the figure), and at most two arcs otherwise (Δ_2 in the figure). Any of the arcs illustrated could degenerate to points if the cone is a ray. (When c is not the center of S, the arc could be the whole circle C.) $\square$

We will need a slight extension of this lemma. Define a *quadrilateral cone* $Q_c(a, b)$ to be the closure of $\Delta_c(a, b) \backslash t$, where t is the triangle determined by (a, b, c). Thus $Q_c(a, b)$ is all the points on the rays from c at or beyond ab. The next lemma says that the conclusion of the previous lemma holds for quadrilateral cones as well.

Lemma 4. *The intersection of a quadrilateral cone $Q_c(a, b)$ with a $(d-1)$-sphere S in $\mathbb{R}^d$ consists of at most two connected components—and, if c is the center of S, of at most one component—each of which is a circular arc or a point.*
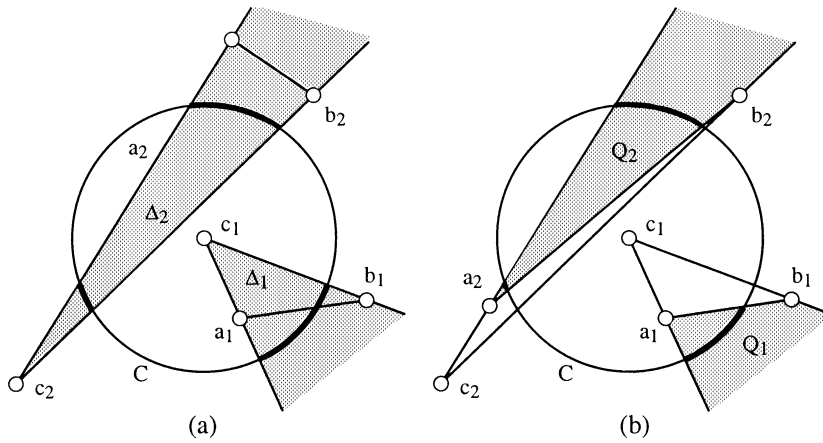
Fig. 2. (a) Intersections of triangle cones $\Delta_1 = \Delta_{c_1}(a_1, b_1)$ and $\Delta_2 = \Delta_{c_2}(a_2, b_2)$ with a circle C centered at c_1. (b) Intersections of quadrilateral cones Q_1 and Q_2 with C.

Proof. As Fig. 2(b) makes clear, $Q_c(a, b)$ is just $\Delta_c(a, b)$ intersected with a closed halfplane in H containing ab. Intersecting the components from Lemma 3 with a halfplane cannot increase their number, and so the claim follows.   □

Obstruction diagram $\text{Ob}(v_0)$. Let $\mathcal{C}_0$ be the *configuration space* for vertex v_0 when v_1 is fixed: the set of all possible positions for v_0 that preserve the length of $v_1 v_0$. $\mathcal{C}_0$ is a 3-sphere S in $\mathbb{R}^4$ centered at v_1 with radius ℓ_0. Let $\mathcal{F}_0$ be the *free space* for vertex v_0 with all other vertices v_i of the chain fixed: the subset of $\mathcal{C}_0$ for which the chain is simple, i.e., for which s_0 does not intersect s_i, $i > 1$, and s_0 intersects s_1 only at v_1. We define the *obstruction diagram* $\text{Ob}(v_0)$ for v_0 as the set such that $\mathcal{F}_0 = \mathcal{C}_0 \backslash \text{Ob}(v_0)$. Our goal is to describe, and ultimately construct, $\text{Ob}(v_0)$.

   To ease notation, let $_j\Delta_i = \Delta_{v_j}(v_i, v_{i+1})$ be the triangle cone with apex v_j determined by segment i, and define $_j Q_i \subseteq {_j\Delta_i}$ as the similar quadrilateral cone.

Lemma 5. *The set of points* $\text{Ob}(v_0) \subset \mathcal{C}_0$ *in the 3-sphere S consists of at most $n - 1$ components, each of which is a circular arc of a circle or a point.*

Proof. $\text{Ob}(v_0)$ is the union of the obstructions contributed by each segment s_i, $i > 1$, plus the single point disallowing overlap with s_1. If s_0 intersects s_i, then v_0 lies in the set $_1 Q_i$ in $\mathbb{R}^4$, for then v_0 lies on a ray from v_1 along s_0, beyond the crossing with s_i. (For example, in Fig. 2(b), we have $c_1 = v_1$, $a_1 = v_i$ and $b_1 = v_{i+1}$.) Thus $_1 Q_i \cap S$ is precisely the locus of positions of v_0 for which s_0 intersects s_i. By Lemma 4, this intersection is a circular arc or a point. Unioning over all $i > 1$ establishes the claim.   □

   The following lemma is now immediate.

Lemma 6. *If v_0's goal position v_g is free, then v_1 may be straightened.*

Proof. Because v_g is free, $v_g \notin \text{Ob}(v_0)$. Because the given chain is assumed simple, the initial position $v_0 \notin \text{Ob}(v_0)$. The locus of possible v_0 positions forms the 3-sphere S. The obstacles $\text{Ob}(v_0)$ are a finite

set of circular arcs and points. The removal of $\text{Ob}(v_0)$ from S^3 cannot disconnect v_0 from v_g. This follows from the fact that $\mathbb{R}^d$ cannot be separated by a subset of dimension of less than or equal to $d - 2$ [13, Theorem 3-61, p. 148]. Neither then can $\mathbb{S}^d$ be so disconnected. For suppose set X disconnects two points p and q of $\mathbb{S}^d$. Then stereographically project $\mathbb{S}^d$ to $\mathbb{R}^d$, from a center not in X or at the two points. This produces a set X' that disconnects p' from q' in $\mathbb{R}^d$, contradicting the quoted theorem.

Therefore there is a path in $\mathcal{F}_0 = S \backslash \text{Ob}(v_0)$ from v_0 to v_g, which represents a continuous motion of s_0 that straightens v_1. $\quad\square$

It is this lemma which justifies the claim made in Section 1.2 that there can be no cages in 4D. We will defer to Section 2.1.3 construction of the path guaranteed by this lemma.

2.1.2. Step 2: s_g is intersected

If s_g is intersected, then rotating s_0 to the goal position necessarily violates simplicity at the goal position. In this case, we slightly move v_1, the joint between s_0 and s_1, so that the new goal position s_g' is no longer intersected. That we can "break" the degeneracy of an intersected goal is established by this lemma:

Lemma 7. v_1 *may be moved to* v_1' *while keeping all other vertices fixed, so that the chain remains simple, and the new goal* s_g' *is not intersected.*

Proof. Fix the positions of $v_0, v_2, v_3, \ldots, v_n$. The 2-sphere

$$S = \left\{ z \in \mathbb{R}^4 \colon |z - v_0| = \ell_0, \ |z - v_2| = \ell_1 \right\}$$

represents all the possible positions for v_1 that preserve the lengths of its incident links. Note that S consists of the intersection of two 3-spheres. Because we may assume that the angle at v_1 is not already straightened, S does not degenerate to a single point. Thus S is a 2-sphere.

Now we construct an obstruction diagram $\text{Ob}(v_1)$ on S that is a superset of all those positions of v_1 for which (1) the goal position s_g (of s_0) is intersected, or for which (2) the chain (v_0, v_1, v_2) intersects the remaining, fixed chain $(v_2, \ldots, v_n)$. We construct a superset rather than the precise obstruction set because the former is easier but equally effective computationally.

1. Intersected goal positions s_g. A goal segment s_g lies on the ray from v_2 through v_1, for it is exactly those s_g that are straight at v_1. For s_g to intersect s_i, v_1 must lie in $_2\Delta_i$, the triangle cone with apex at v_2 and delimited by s_i. See Fig. 3. Not every $v_1 \in \ _2\Delta_i$ leads to intersection of s_g with s_i: s_g must reach s_i. The relevant subset of $_2\Delta_i$, could be detailed, but because it has one curved edge, we content ourselves with a supset of the obstructions by forbidding v_1 anywhere in $_2\Delta_i$.

   Applying Lemma 3 shows that $S \cap \ _2\Delta_i$ contributes at most two arcs or points to $\text{Ob}(v_1)$, for each $i \notin \{0, 1\}$.

2. Intersections between s_0 and s_1 and the remainder of the chain. $\text{Ob}(v_1)$ also contains all the positions of v_1 that cause the two adjacent links to intersect any of the other segments. The link $v_2 v_1$ is clearly covered by $_2\Delta_i$. The link $v_0 v_1$ can be handled by the analogous triangle cone $_0\Delta_i$ with apex at v_0 and through s_i. Again these sets provide a superset of the obstructions, and Lemma 3 again applies.

Summing over all i yields the obstruction superset $\text{Ob}(v_1)$ composed of at most $2 \cdot 3(n - 2) = \text{O}(n)$ arcs or points on S. Thus $\text{Ob}(v_1)$ is an arrangement of $\text{O}(n)$ arcs on a 2-sphere, with the initial position of v_1 lying on at least one arc (because by hypothesis, s_g is intersected). Choosing any point $v_1' \in S \backslash \text{Ob}(v_1)$ interior to an arrangement cell on whose boundary v_1 lies suffices to establish the claim. $\quad\square$
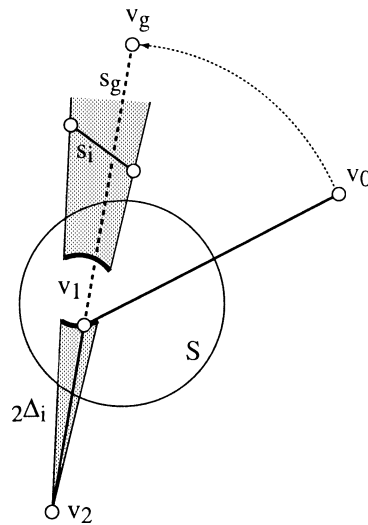
Fig. 3. The triangle cone $_2\Delta_i$ intersects the sphere S in at most two circular arcs.

Note that it is quite possible for v_1 to be confined within a cell of the arrangement $Ob(v_1)$, but that this "cage" is no impediment. We do not need a path from v_1 to an arbitrary point of S; rather we only need a path to any unobstructed point v_1'. Although we could construct the arrangement $Ob(v_1)$ in $O(n^2\alpha(n))$ time and $O(n^2)$ space [10,12], for our limited goal of constructing just one point, we can do better.

Lemma 8. *A move of v_1 to the position guaranteed by Lemma 7 may be computed in* $O(n)$ *time and* $O(n)$ *space.*

Proof. Let $Z = \{a_1, \ldots, a_m\}$ be the collection of arcs of V that contain v_1. Z may be found by a brute force check of each of the $O(n)$ arcs. Pick two arcs a_1 and a_j angularly consecutive about v_1. This can be accomplished in $O(n)$ time by fixing a_1, and letting a_j be the arc that makes the smallest angle with a_1. Let a be a circular arc ray (i.e., a directed great circle starting and ending at v_1) that bisects this angle; or if Z only contains one arc, let a be orthogonal to it; or if Z only contains one point, let a be any ray from v_1.

Intersect a with every arc and point of $Ob(v_1)$, again in $O(n)$ time. Let δ be the distance from v_1 along a to the closest intersection. Finally, choose v_1' as the point $\delta/2$ along a. This point is guaranteed to be off $Ob(v_1)$, and therefore unobstructed.

Moving (in one move) v_1 to v_1' establishes a new goal s_g' that is not intersected.   □

2.1.3. Motion planning

Now that we know we can perform Step 2 of Algorithm 1a in $O(n)$ time per iteration, we return to finding a path through S^3 for v_0, as guaranteed by Lemma 6. Motion planning between two points of the 3-sphere $\mathcal{F}$ may be achieved by any general motion planning algorithm [18, Section 40.1.1]. For example, Canny's Roadmap algorithm achieves a time and space complexity of $O(n^k \log n)$, where n is the number of obstacles and k the number of degrees of freedom in the robot's placements. In our case, $k = 3$. His algorithm produces a piecewise algebraic path through $\mathcal{F}$, of $O(n^k)$ pieces. Each piece constitutes a
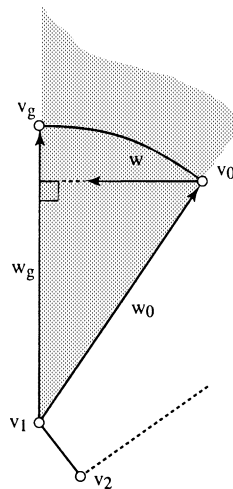
Fig. 4. The goal direction vector w defines the direction that w_0 should be rotated to reach w_g. The shaded triangle cone $_1\Delta(v_0, v_g)$ is not crossed by any links of the chain if w is unobstructed.

constant number of moves, with the constant depending on the algebraic degree of the curves, which is bounded as a function of k. Therefore each joint straightening can be accomplished in $O(n^3)$ moves. Repeating the planning and straightening n times leads to $O(n^4)$ moves in $O(n^4 \log n)$ time. In the next section we reduce the $O(n^3)$ moves per joint straightening to just 3 moves per straightening.

2.2. Algorithm 1b

We have now established Theorem 1, but with weaker complexity bounds than claimed. It is not surprising that applying a general motion planning algorithm is wasteful in our relatively simple situation. In fact a significant improvement over Algorithm 1a can be achieved by switching attention from the absolute position of v_0, to the direction in which s_0 rotates. Let the vector along s_0 be $w_0 = v_0 - v_1$, and similarly let $w_g = v_g - v_1$. Let w be the *goal direction*: a unit vector orthogonal to w_g that represents the direction in which w_0 should be rotated to move it to its goal position. See Fig. 4. Thus w is the unique unit vector pointing in the direction of the component of $w_g - w_0$ orthogonal to w_g:

$$a_1 w_g + b_1 w = w_g - w_0 \tag{7}$$

for some reals $a_1 > 0$ and $b_1 > 0$. The space of possible directions w forms a 2-sphere rather than the 3-sphere we faced in Step 1 of Algorithm 1a. This permits replacing the $O(n^3 \log n)$ moves per step from motion planning, with at most two moves. We now proceed to describe this. Because this represents a computational improvement only, the proofs are only sketched. More detailed proofs are contained in [6].

Algorithm 1b distinguishes three possibilities.
1. The goal position is *intersected* by some other link of the chain (just as in Algorithm 1a).
2. The goal direction is *obstructed* in that rotation of s_0 in the direction w might hit some link of the chain along its direct rotation to the goal position. We again define a direction to be obstructed conservatively, working with a superset of the true obstructions: w is obstructed if the triangular cone $\Delta_{v_1}(v_0, v_g) = {}_1\Delta(v_0, v_g)$ is intersected by any s_i, $i > 1$.
3. The goal direction is *free*: it is not obstructed (and so the goal position is not intersected).

A high-level view of our second algorithm is as follows.

Algorithm 1b. Open chains
repeat until chain straightened do
    1. if w is *free* then
       Rotate s_0 directly to s_g.
    2. else if w is *obstructed* then
       Rotate s_0 to new position whose goal direction is free.
    3. else if s_g is *intersected* then
       Move v_1 so that the goal position is not intersected.

Step 3 is identical to Step 2 of Algorithm 1a, so we only discuss the first two steps.

2.2.1. Step 1: w is free

By our definitions, s_0 may be rotated directly to s_g without hitting any other segment of the chain. Because the goal position s_g is not intersected, the chain remains simple even after the rotation has been completed. Therefore, the link s_0 can be straightened in one move.

Note that this is the generic situation, in that for a "random" chain, e.g., one whose vertex coordinates are chosen randomly from a 4D box, each link can be straightened with Step 1 of the algorithm with probability 1. Steps 2 and 3 handle "degenerate" cases. We exploit this in our implementation (Section 2.3).

2.2.2. Step 2: w is obstructed (but s_g is not intersected)

Detecting obstructions. When w is obstructed, we again rely on construction of an obstruction diagram. First we describe the space in which the obstruction diagram is embedded.

Consider the space of possible directions from which s_0 might approach s_g. In 3D, this set of unit vectors forms a 1-sphere, a circle, which can be viewed as orthogonal to s_g and centered at v_g; see Fig. 5(a). Similarly, in 4D, the set of possible approach directions toward s_g forms a unit 2-sphere S, which again we center on v_g. Every point on this sphere represents a direction of approach to s_g; see Fig. 5(b).

The *obstruction diagram* $\mathrm{Ob}(s_g)$ is the set of vectors w representing obstructed goal directions for s_g.

Lemma 9. *If the goal s_g is not intersected, the obstruction diagram* $\mathrm{Ob}(s_g)$ *consists of at most n arcs on S.*

Proof. Take an arbitrary segment s_i of the chain, and "project" it to s_i' in the 3-flat $\Pi \supset S$ orthogonal to s_g; i.e., $s_i' = {}_1\Delta_i \cap \Pi$. See Fig. 5(a) for the 3D analog. We first claim that the set of directions w obstructed by s_i' is identical to those obstructed by s_i. Next we determine this set of directions. Every vector w determined by a point on S and its center v_g, is orthogonal to s_g by our choice of Π. So the set of w obstructed by s_i' is just those w determined by the intersection of ${}_g\Delta(s_i')$ with S. By Lemma 3, this is at most one arc on the sphere. See Fig. 6. □

Detection of obstruction therefore reduces to deciding if w lies on one or more arcs of an arrangement of circular arcs on a 2-sphere S, which can be accomplished in $\mathrm{O}(n)$ time and space as in Lemma 8.
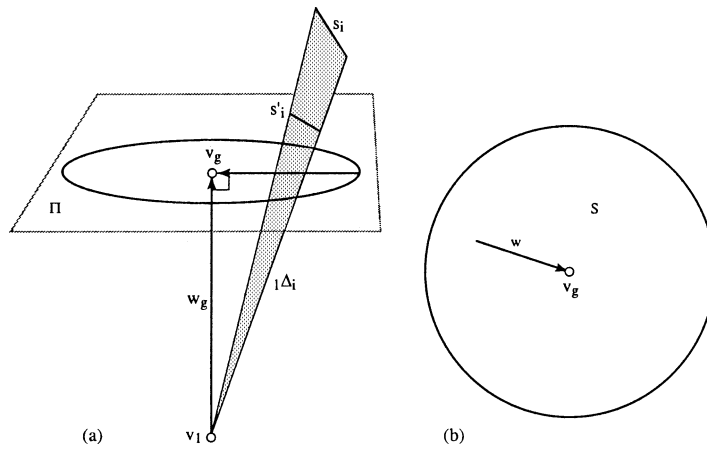
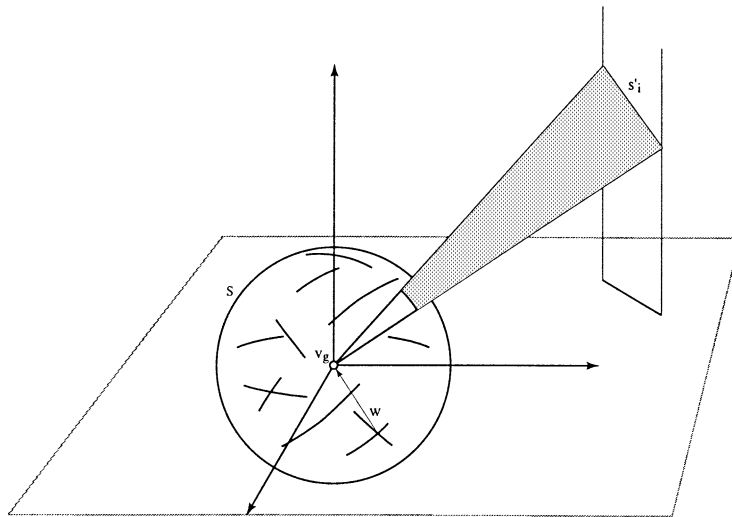Fig. 5. (a) Directions approaching the goal position in 3D. (b) S is a 2-sphere in $\mathbb{R}^4$.

Fig. 6. In 4D, s_i projects to s_i' in the 3-flat containing S, and produces an arc of the obstruction diagram determined by the intersection of the triangle cone $_g\Delta(s_i')$ with S.

Skirting obstructions. Our next task is to move s_0 when w is obstructed so that its new goal direction is free. This task is similar to that handled in Lemma 8—stepping off the arcs meeting at w—with one additional constraint: the move must maintain the simplicity of the chain. Note that $\mathrm{Ob}(s_g)$ does not record chain simplicity, but rather records free goal directions. So we need to find a Δw that will move w to be free, while simultaneously maintaining simplicity during the motion of s_0.

Lemma 10. *If w is obstructed, s_0 can be moved, maintaining simplicity throughout, so that its new goal direction $w' = w + \Delta w$ is unobstructed. Δw may be computed in $\mathrm{O}(n)$ time and space.*

Proof. Because the chain is initially simple, there must exist a $\beta > 0$ such that rotation of s_0 about v_1 by an angle less than β leaves the chain simple. This β can be computed by finding the smallest distance d from s_0 to any other segment, and using the angle of a cone centered at s_0 of radius $d/2$. Now Δw is selected just as in Lemma 8, but subject to this angle constraint. $\square$

Note that because we have based our analysis on a fixed s_g, moving s_0 does not alter the obstruction diagram, which records obstructed directions of approach to s_g.

2.2.3. Algorithm 1b complexity

The algorithm straightens one joint in at most three moves: one to move v_1 so the goal is not intersected (Step 3), one to move v_0 so that the goal is not obstructed (Step 2), and one to rotate directly to the goal (Step 1). The total number of moves used by the algorithm is then at most $3n = O(n)$. For each of the n iterations, Lemma 10 shows that the computations can be performed in linear time and space. This then establishes the total time complexity of $O(n^2)$ claimed in Theorem 1. Because each move is performed independently, the obstruction diagram arcs may be discarded after each iteration. Thus the space requirements remain at $O(n)$.

2.3. Implementation

We have implemented Algorithm 1b for chains in "general position" in C++. The program accepts a chain as input, and first checks if it is simple. If it is, the straightening process starts; otherwise the program exits. The program then straightens the chain link-by-link using Step 1, one move per link. It also detects whether the goal is obstructed (Step 2) or intersected (Step 3) by solving sets of linear equations, but in those cases it simply halts; we have not implemented the obstruction diagrams, or avoiding obstructions. For a chain whose vertex coordinates are chosen randomly, the program straightens it with probability 1, for then the degenerate cases handled by Steps 2 and 3 (when a point, w or v_1, hits an
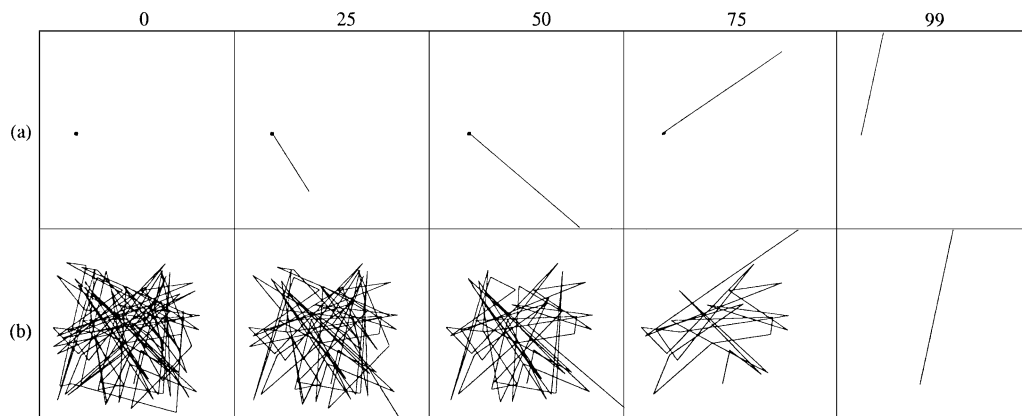

Fig. 7. Snapshots of the algorithm straightening a chain of $n = 100$ vertices, initially (0), and after 25, 50, 75 and all 99 joints have been straightened (left to right). (a) Scale approx. 50:1; the entire chain is visible in each frame. (b) Scale approx. 1:1; the straightened tail is "off-screen". (The apparent link length changes are an artifact of the orthographic projection of the 4D chain down to 2D.)

arc on a 2-sphere, e.g., Fig. 6) are unlikely to occur. The output of the program is a set of Geomview or Postscript files that animate the straightening process. Fig. 7 shows output for a chain whose $n = 100$ vertices were chosen randomly and uniformly in $[0, 1]^4$.

3. Straightening trees in 4D

It will come as no surprise that essentially the same algorithm as just described can straighten trees in 4D. The reason is that each segment was considered a fixed obstruction in the chain straightening algorithm, and whether those segments form a chain or a tree is largely irrelevant, as long as there is a free end. There is one spot at which the difference between a chain and a tree does matter, however: freeing up an intersected goal position. We concentrate on this difference in the description below.

Algorithm 2. Trees
repeat until straightened do
    1. Identify a node x with chain descendants C.
    2. Straighten each chain in C, forming C'.
    3. if r_g is intersected then
       Construct obstruction diagram $\mathrm{Ob}(x)$ on 2-sphere.
       Move x so that r_g not intersected.
    4. Rotate each segment in C' to r_g and coalesce.

Algorithm 2 chooses a leaf z of the given tree T as root, and then identifies some node x all of whose descendant subtrees are chains (Step 1). Call this set C, see Fig. 8(a). Each chain in C can be straightened one at a time via Algorithm 1, leaving a set of straightened chains, or segments, C' (Step 2). Define the goal ray to be the extension of the parent segment yx incident to x; see Fig. 8(b). If r_g is not intersected by any segment of $T \setminus C'$, then each segment in C' can be rotated to r_g, each lying on top of one another (Step 4). We can view them as coalesced into a single link, reducing the degree of x to 2. The process then repeats.

If, however, r_g is intersected (Step 3), we need to move x so that the goal ray becomes free. There are several ways to achieve this; we choose to parallel Step 2 of Algorithm 1a. Let $(v_0, v_1, \ldots, v_m)$ be one of the chains of C', with v_m adjacent to x. We distinguish this chain from the others in C'; call the set of others C_1'. Let the 2-link chain (v_0, x, y) play the role of (v_0, v_1, v_2) in Algorithm 1a. In that algorithm we argued that $\mathrm{Ob}(v_1)$ is a set of arcs and points on a 2-sphere (Fig. 3). Here we will reach the same conclusion for $\mathrm{Ob}(x)$ on the 2-sphere S of positions for x.

The only difference is that in the current situation, the *star* of segments C_1' is attached to x, and we need to augment $\mathrm{Ob}(x)$ to reflect its obstructions. We opt to translate C_1' as x moves; this gives rise to two sets of constraints: (1) those caused by a segment in C_1' intersecting a segment of $T' = T \setminus \{C_1' \cup xy \cup xv_0\}$; (2) those caused by xy or xv_0 intersecting a segment in C_1'. For the first, the locus of positions of x that cause some $s \in C_1'$ to intersect some $s_i \in T'$ is a parallelogram, congruent to the Minkowski sum $s \oplus s_i$. Analogous to Lemma 3, it is easy to see that this holds:

Lemma 11. *The intersection of a parallelogram with a $(d-1)$-sphere S in $\mathbb{R}^d$ consists of at most four connected components, each of which is an arc or a point.*
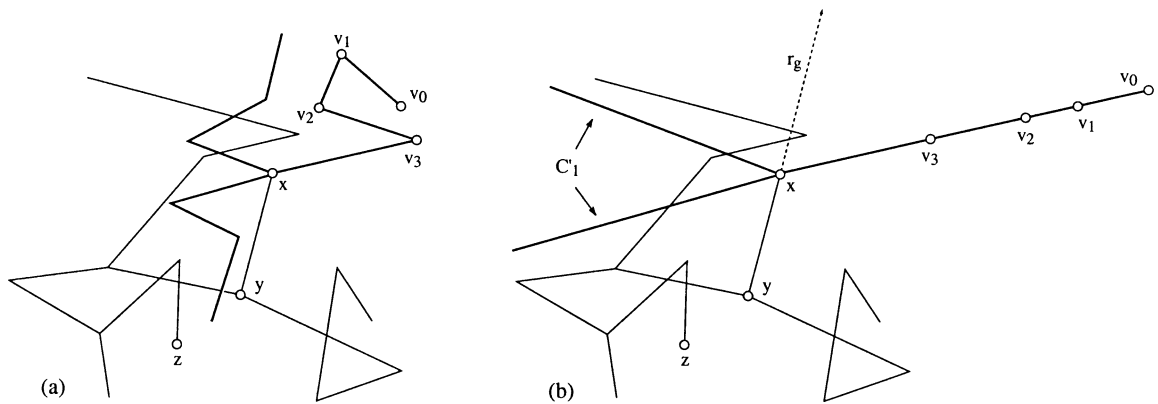
Fig. 8. (a) Tree T rooted at z. (b) After straightening chains C incident to x; C_1' is the set of straightened chains excluding one distinguished chain $(v_0, v_1, \ldots)$.

Thus the constraints (1) add $O(n)$ arcs or points to $Ob(x)$. Constraints (2) can be seen to consist of $O(n)$ points on S: translating the star C_1' to y determines the rays that xy might align with to cause xy to intersect C_1'; and similarly translating C_1' to v_0 determines rays for intersection with xv_0. The two placements of C_1' therefore generate $O(n)$ additional point obstructions.

With $Ob(x)$ again a set of $O(n)$ arcs and points on a 2-sphere, Lemmas 7 and 8 hold, leading to the same time complexities claimed for Algorithm 1, and establishing Theorem 2.

4. Convexifying closed chains in 4D

Our algorithm for convexifying closed chains employs the *line tracking* motions introduced in [14]. Indeed our algorithm mimics theirs in that we repeatedly apply line tracking motions, each of which straightens at least one joint, until a triangle is obtained (which is a planar convex polygon, as desired). Although the overall design of our algorithm is identical, the details are quite different, for there is a major difference with [14]: They permitted self-intersections of the chain, whereas we do not. This greatly complicates our task. [4]

Let $(v_0, v_1, v_2, v_3, v_4)$ be five consecutive vertices of a closed polygonal chain. We allow $v_0 = v_4$. A *line tracking* motion of v_2 moves v_2 along some line L in space, while keeping both v_0 and v_4 fixed. As long as the angle at joints v_1 and v_3 (the *elbows*) are neither π (straight) nor 0 (folded), such a motion is possible. Neither angle can be 0 because that would violate the simplicity of the chain. Straightening one joint is precisely our goal, so we assume that neither joint is straight; and therefore a line tracking motion is possible.

We will choose L and a direction along it so that the movement increases the distance from v_2 to both v_0 and v_4 simultaneously. This necessarily opens both elbow angles. The motion stops when one elbow straightens. The only issue is whether this can be done while maintaining simplicity. Our aim is to prove this theorem:

---

[4] An alternative convexifying algorithm, again permitting self-intersections, is described in [16]. Sallee accomplishes the same result by a different basic motion, involving four consecutive vertices rather than the five used in [14].

Theorem 6. *For a simple 4D chain* $(v_0, \ldots, v_4)$*, there exists a line tracking motion of* v_2 *that straightens either* v_1 *or* v_3 *(or both) while maintaining simplicity of the chain throughout the motion.*

A high-level view of the algorithm is as follows:

Algorithm 3. Closed chains
repeat until chain is a triangle do
    Compute a line L along which to move v_2.
    Compute free paths π_1 and π_3 for v_1 and v_3.
    Move v_2 along L, v_1 along π_1, and v_2 along π_2.
    Freeze the straightened joint v_1 or v_3.

4.1. Choosing L

To fix L, the ray along which v_2 moves, we choose a point $q \in \mathbb{R}^4$ different from v_2, and let L be the ray from v_2 that contains v_2q. We will choose q so that it is itself the point where one of the two joints v_1 or v_3 becomes straight while moving v_2 along L.

Lemma 12. *A point q determining an appropriate L may always be found, and in time and space* $\mathrm{O}(n^4)$*.*

Proof. We choose q so that it satisfies these conditions:
1. Moving v_2 along L increases the distance from v_2 to v_0 and to v_4.
2. Either v_1 or v_3 becomes straight, i.e., $|qv_0| = |v_0v_1| + |v_1v_2| = r_0$, or $|qv_4| = |v_2v_3| + |v_3v_4| = r_4$.
3. (a) If $|qv_0| = r_0$, then qv_0 does not intersect any other segment of the chain than those to which it is incident.
    (b) If $|qv_4| = r_4$, then qv_4 does not intersect any other segment of the chain than those to which it is incident.
4. v_2q does not intersect a segment s_i, $i > 4$.
Condition 3 ensures that our "goal" is not itself intersected, in the sense used in Section 2.

Let R_i be the set of points (the "region") of $\mathbb{R}^4$ that satisfy condition 1 above. R_1 is the intersection of two closed half-spaces containing v_2, orthogonal to v_0v_2 and v_2v_4, respectively. Note that $v_2 \in R_1$. If v_0v_2 and v_2v_4 lie on the same line, R_1 degenerates to a 3-flat orthogonal to that line; otherwise it is a 4-dimensional set. [5] See Fig. 9 for a lower dimensional analog of the situation.

The set of points $R_2 = S_0 \cup S_4$ in 4D that satisfy condition 2 is the union of two 3-spheres, S_0 and S_4, centered at v_0 and v_4 and of radius r_0 and r_4, respectively. Because $|v_0v_2| < r_0$, v_2 is inside the 4-ball bounded by S_0. Therefore, $R_1 \cap S_0 \neq \emptyset$. Similarly, $R_1 \cap S_4 \neq \emptyset$. So $R_1 \cap R_2 \neq \emptyset$. The dimensionality of this set depends on whether or not $\{v_0, v_2, v_4\}$ are collinear: if they are, the 3-spheres are intersected by a 3-flat producing 2-spheres; if they are not, the 3-spheres are intersected by a 4-dimensional wedge, producing 3-dimensional regions of the 3-spheres.

Consider condition 3(a); clearly 3(b) is analogous. We want all those points q such that qv_0 does not intersect any other link of the chain. Clearly the points forbidden by segment s_i lie in the triangle cone $_0\Delta_i = \Delta_{v_0}(v_i, v_{i+1})$, just as in the proof of Lemma 7. Intersecting $_0\Delta_i$ for all i with $R_1 \cap R_2$ marks the

---

    [5] Although we could remove this possible degeneracy by moving v_2 in a neighborhood (while preserving simplicity) to break the collinearity, this is not necessary, as the proof goes through regardless.
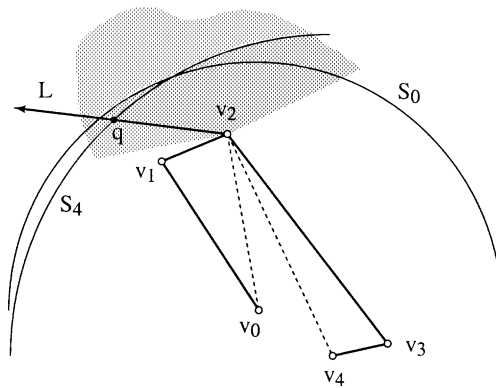
Fig. 9. Choosing $q \in L$. $R_1 \cap R_2 = R_1 \cap (S_0 \cup S_4)$.

set of points that must be avoided in our choice of q: $R_3 \supset \mathbb{R}^4 \setminus \bigcup_i {}_0\Delta_i$. It is easiest to concentrate on the intersection of ${}_0\Delta_i$ with the spheres in R_2. By Lemma 3, we know this intersection is at most two arcs or points, independent of the dimension of the spheres. So whether or not $\{v_0, v_2, v_4\}$ are collinear, the intersection produces O(n) arcs or points. Similarly, condition 4 leads to $R_4 \supset \mathbb{R}^4 \setminus \bigcup_{i>4} {}_2\Delta_i$, for $v_2 q$ can intersect s_i only if q lies in ${}_2\Delta_i$. Again, O(n) arcs or points need be avoided in $R_1 \cap R_2$. No union of arcs and points can cover the set $R_1 \cap R_2$, which is either 2- or 3-dimensional. Thus $\bigcap_i R_i \neq \emptyset$. We need only choose a q in this set.

There are a variety of ways to choose such a q algorithmically. A naive method is to first construct an arrangement of 2-flats in $\mathbb{R}^4$ each containing a triangle ${}_0\Delta_i$ or ${}_2\Delta_i$. This computation could be performed in O(n^4) time and space [11]. Intersecting this arrangement with the halfspaces delimiting R_1 and the 3-spheres S_0 and S_4 leave us cells bound by algebraic surfaces inside $\bigcap_i R_i$. The centroid of any such cell can be selected as q. □

4.2. Line tracking in 3D

We start by thinking about the analogous situation in 3D. This will both set notation, and ground intuition by showing why Theorem 6 does not hold in 3D.

4.2.1. Topology of configuration space in 3D

Let $\mathbb{R}_{[0,1)}$ be the interval $[0, 1)$ on the real line, open at 1. We will parameterize the location of v_2 along L by $t \in [0, 1)$, with $t = 0$ the start, and $t = 1$ when v_2 reaches the q of Lemma 12, the first time at which a joint, straightens. Let this joint be v_1 without loss of generality. Let $\mathcal{C}'$ be the configuration space of the four-link system in isolation, permitting intersections between the links, the prime to remind us that $t = 1$ has been excluded. We claim that

$$\mathcal{C}' = \mathbb{S}^1 \times \mathbb{S}^1 \times \mathbb{R}_{[0,1)}. \tag{8}$$

This can be seen as follows. Fix some t so that v_2 is fixed. Then each of v_1 and v_3 is free to rotate (independently) on a circle in $\mathbb{R}^3$ centered on the axis $v_0 v_2$ and $v_2 v_4$, respectively. As t varies from 0 to 1, these circles move in space, and grow and shrink in radius; see Fig. 10. At $t = 1$ the v_1 circle shrinks to a point.
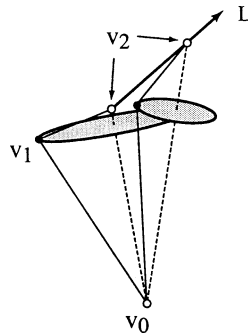
Fig. 10. In 3D, the circle on which v_1 may lie moves in space as v_2 slides up L.

But for $t \in [0, 1)$, both circles retain a positive radius. Thus the configuration space $\mathcal{C}$ has the topology of $\mathbb{S}^1 \times \mathbb{S}^1$ for each t, and the claim follows.

4.2.2. Obstruction diagram in 3D

As in Section 2, we incorporate the obstacles representing the other links via an "obstruction diagram". We start by ignoring the four moving links as obstructions, and only consider the remaining, fixed links of the polygonal chain as obstacles. We develop the obstruction diagram first for fixed t, so that the relevant configuration space is $\mathbb{S}^1 \times \mathbb{S}^1$. Because we are ignoring the moving links as obstructions, movement on the two circles is independent, so it suffices to determine the obstruction diagram $\mathrm{Ob}(v_1)$ on one 1-sphere/circle S_1, that for v_1. The following lemma will be key in 4D.

Lemma 13. *In 3D, if $(v_2 - v_0) \cdot (v_1 - v_0) \neq 0$ and $(v_2 - v_0) \cdot (v_1 - v_2) \neq 0$, then a single segment contributes at most four points to $\mathrm{Ob}(v_1)$. Otherwise, if either dot product is zero, a segment could obstruct a finite-length arc of the S_1 circle for v_1.*

Proof. We only sketch a proof, leaving details for the 4D case considered below. Spinning v_1 along its circle of freedom while maintaining v_0 and v_2 fixed traces out a "spindle" shape, which can be viewed as the union of two cones. A segment s that does not lie along a line through either v_0 or v_2 can intersect each cone in at most two points, and so intersect the spindle in at most four points. See Fig. 11. These four segment-cone intersection points correspond one-to-one with four v_1 positions on S_1 at which there is an intersection between the 2-link chain (v_0, v_1, v_2) and s.

If the segment s lies in the surface of the cone, then it contributes just one point to the diagram, corresponding to the angle of spin that aligns one of the two links with the obstacle segment.

Finally, if either of the two links $v_0 v_1$ or $v_1 v_2$ is orthogonal to the axis of the spindle, i.e., either dot product is zero, then a segment obstacle could obstruct the entire circle, for one of the cones is then degenerately flat. As Fig. 12 illustrates, here a segment might obstruct a range of rotations of $v_1 - v_2$, producing an arc in $\mathrm{Ob}(v_1)$. $\square$

4.2.3. Disconnected free space in 3D

Let $v_1(t)$ represent the position of v_1 on its circle S_1 at a particular time t. The goal is for the links (v_0, v_1, v_2) to avoid all obstacles, which means that $v_1(t)$ should avoid points of the obstruction diagram. If we ignore for now the orthogonality case, then we have the situation that a finite set of links produce
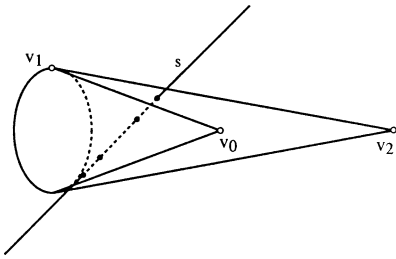
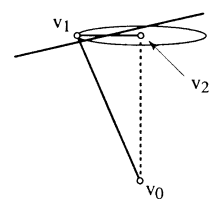Fig. 11. One segment s can contribute four points to $Ob(v_1)$.

Fig. 12. $(v_2 - v_0) \cdot (v_1 - v_2) = 0$ and segment s (which lies in the plane of the circle) contributes an arc to the obstruction diagram $Ob(v_1)$.
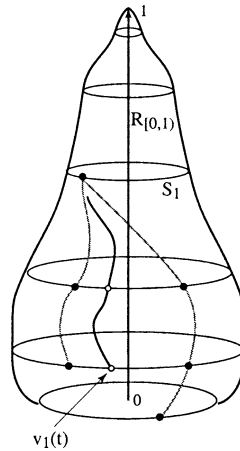

Fig. 13. Point $v_1(t)$ is "captured" by two obstacle points in configuration space, the tube-like surface.

an obstruction diagram consisting of a finite set of points on S_1. As t moves, these points wander around the circle, disappear, enter, join or split. The moving links, previously ignored, just add a few more points to the obstruction diagram, moving in a different manner. The diagram for the configuration space for v_1 then looks like arcs on the tube-like $\mathbb{S} \times \mathbb{R}_{[0,1)}$. It is clear that it is possible for the point $v_1(t)$ to be "captured" between two points of the obstruction diagram which move together and squeeze $v_1(t)$ into a collision. See Fig. 13. In this case, the free space for the point v_1 is not connected from $p_1(0)$ to $p_1(1)$. And indeed, it is easy to "cage in" the moving links by the fixed links so that no straightening is possible. Our next task is to show that such caging-in is impossible in 4D.

4.3. Line tracking in 4D

4.3.1. Topology of configuration space in 4D

Turning now to 4D, exactly analogous to the situation in 3D, an elbow at the join of two links has a space of possible motions in 4D that is topologically $\mathbb{S}^2$, for it is the intersection of two 3-spheres. Thus the configuration space $\mathcal{C}'$ of our four-link chain for $t \in [0, 1)$, ignoring self-intersections, is

$$\mathcal{C}' = \mathbb{S}^2 \times \mathbb{S}^2 \times \mathbb{R}_{[0,1)}. \tag{9}$$

At $t = 1$ at least one of the 2-spheres shrinks to a point.

4.3.2. Obstruction diagram in 4D

As in 3D, we analyze the obstruction diagram on one 2-sphere S_1, that for v_1, at a fixed value of t: $\mathrm{Ob}(v_1)$. Let $v_1(t)$ represent the position of v_1 on its sphere S_1 at time t. We seek the set of points $\mathrm{Ob}(v_1)$ for which the links (v_0, v_1, v_2) intersect some other segment of the chain, $s_4, s_5, \ldots, s_n$. Just as in 3D, $\mathrm{Ob}(v_1)$ is (in nondegenerate situations) a finite set of points. This claim relies on how a line may intersect a cone.

Define a $(d-1)$-*cone* $C(a, b, \theta)$, for apex point a, axis point b and cone angle $\theta \in [0, \pi/2]$, to be the set of points $p \in \mathbb{R}^d$ that form an angle θ with respect to the axis, i.e., which satisfy

$$(p - a) \cdot (b - a) = |p - a||b - a| \cos\theta. \tag{10}$$

For the extreme values of θ, $C(a, b, 0)$ is a ray from a through b, and $C(a, b, \pi/2)$ is a $(d-1)$-flat containing a and orthogonal to ab. Note that a 1-cone is not the triangle cone from Section 2.1.1; rather a 1-cone is the union of two rays from a. In 3D, $C(a, b, \theta)$ is the surface of a right circular cone whose axis is the ray from a through b, and which form the angle θ with the axis at a (cf. Fig. 11). Its intersection with a plane orthogonal to ab is a circle. In 4D, $C(a, b, \theta)$ is a "right spherical cone", whose intersection with a 3-flat orthogonal to ab is a 2-sphere. Note that it is no restriction to insist that $\theta \in [0, \pi/2]$, for we can ensure this for $\theta > \pi/2$ by selecting an axis point b' for the cone to be on the other side of the apex a, on the line containing ab, thereby "reflecting" θ to $\pi - \theta$.

Lemma 14. *The intersection of the $(d-1)$-cone $C(a, b, \theta)$, $\theta \neq \pi/2$, with a line, ray or segment whose containing line does not include the apex a, is at most two points*: *two points, one point or empty.*

This claim can be seen intuitively as follows. Let C be the cone and s a segment in $\mathbb{R}^d$. If s is contained in a $(d-1)$-flat Π orthogonal to ab, then because $\Pi \cap C$ is a sphere, the result follows from Lemma 2. Otherwise s is contained in a flat whose intersection with C is an ellipsoid, and the result follows because an ellipsoid is affinely equivalent to a sphere [17, p. 95].

Proof. Let $|ab| = 1$ without loss of generality. Translate and rotate C so that $a = (0, 0, \ldots, 0)$ and $b = (1, 0, 0, 0, \ldots, 0)$. For a point $p = (x_1, \ldots, x_d)$, Eq. (10) reduces to

$$p \cdot b = |p| \cos\theta, \tag{11}$$

$$(x_1, \ldots, x_d) \cdot (1, 0, 0, 0, \ldots, 0) = \sqrt{x_1^2 + \cdots + x_d^2}\, \cos\theta, \tag{12}$$

$$x_1^2 = (x_1^2 + \cdots + x_d^2) \cos^2\theta. \tag{13}$$

Represent the point p via the parameter t:

$$p = (\alpha_1 + \beta_1 t, \ldots, \alpha_d + \beta_d t). \tag{14}$$

Substitution of this into Eq. (13) yields a quadratic equation in t, which has at most two roots.

We now examine the degenerate solutions. Because we assumed that $\theta \neq \pi/2$, $\cos\theta \neq 0$. Thus the right hand side of Eq. (13) can only be zero when $x_1^2 + \cdots + x_d^2 = 0$, i.e., when $p = (0, 0, \ldots, 0)$ is the apex a. This corresponds to a line through a, excluded by our assumptions.   □

Lemma 15. *In 4D, if $(v_2 - v_0) \cdot (v_1 - v_0) \neq 0$ and $(v_2 - v_0) \cdot (v_1 - v_2) \neq 0$, then a single segment s contributes at most four points to $\mathrm{Ob}(v_1)$.*

Proof. Moving v_1 sweeps out two finite cones, which are truncations of the infinite cones $C(v_0, v_2, \theta_0)$ and $C(v_2, v_0, \theta_2)$, with

$$(v_2 - v_0) \cdot (v_1 - v_0) = |v_2 - v_0||v_1 - v_0| \cos \theta_0, \tag{15}$$

$$(v_2 - v_0) \cdot (v_1 - v_2) = |v_2 - v_0||v_1 - v_2| \cos \theta_2. \tag{16}$$

By the preconditions of the lemma, we have $\theta_j \neq \pi/2$, $j = 0, 2$, so we may assume $\theta_j \in [0, \pi/2)$ by the reflection maneuver suggested previously. Consider two cases:

1. The line containing s does not pass through either cone apex, v_0 or v_2. The conditions of Lemma 14 are satisfied, establishing that s intersects the two cones in at most four points. Each of these points fixes a position of v_1 corresponding to an obstruction, and so contributes this point to $Ob(v_1)$.

2. The line H containing s passes through v_0 (the case through v_2 is exactly analogous and will not be treated separately). Then it may be that $s \cap C(v_0, v_2, \theta_0)$ is a subsegment of s. This is because the vector $p - v_0$ makes the same angle with $v_2 - v_0$ for all $p \in s$ (cf. Eq. (10)). In this case, s obstructs the unique position of v_1 that places it on H, and so contributes just one point to $Ob(v_1)$. Together with the at most two points from the other cone, s generates at most three points of $Ob(v_1)$. □

The case excluded by the precondition of Lemma 15 refers to the situation in which one cone is degenerately flat, as previously illustrated in Fig. 12. We now analyze this situation in detail.

Lemma 16. *If $(v_2 - v_0) \cdot (v_1 - v_0) = 0$, then $Ob(v_1)$ is a finite set of points and arcs on S_1 (the 2-sphere of v_1 positions).*

Proof. In this case $\theta_0 = \pi/2$ from Eq. (15), and the infinite cone $C(v_0, v_2, \pi/2)$ degenerates to the 3-flat orthogonal to the axis $v_0 v_2$ and including the apex v_0. The finite cone swept out by the link $s_0 = v_0 v_1$ is a ball B_0 of radius ℓ_0 centered at v_0. In the 3D situation, B_0 is a disk (cf. Fig. 12); in 4D, it is a solid sphere whose boundary is a 2-sphere S_1 representing the possible positions for v_1.

The obstructed positions on S_1 are those for which s_0 intersects some segment s_i. Consider two possibilities:

1. s_i does not lie in the same 3-flat of $\mathbb{R}^4$ as S_1. Then s_i intersects B_0 in at most one point p (because it can intersect the flat in at most one point), and then only when s_0 passes through p do we have an obstruction. Thus s_i contributes one point to $Ob(v_1)$.

2. s_i is in the same 3-flat as S_1. Now we have a situation exactly analogous to that shown in Fig. 6: the obstruction is the intersection of the triangle cone $_0\Delta_i$ with S_1. Lemma 3 then establishes that s adds at most two arcs or points to $Ob(v_1)$. □

Lemma 17. *The condition $(v_2 - v_0) \cdot (v_1 - v_0) = 0$ can hold at most one value of $t \in [0, 1]$ during the movement of v_2 along L.*

Proof. This follows immediately from our choice of L, which guarantees that the distance $|v_0 v_2|$ increases, and so the angle at v_1 opens. This angle can therefore pass through $\pi/2$ at most once. See Fig. 14. □
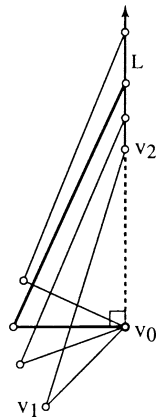
Fig. 14. The special condition $(v_2 - v_0) \cdot (v_1 - v_0) = 0$ holds at most once.

4.3.3. Connected free space in 4D

Again let $v_1(t)$ represent the position of v_1 on its 2-sphere S_1 of possible positions. We first describe the free space for the motion of the 2-link chain (v_0, v_1, v_2), avoiding the fixed links $s_4, s_5, \ldots, s_n$. It is a subset of $\mathbb{S}^2 \times \mathbb{R}_{[0,1)}$. For each $t \in [0, 1)$, we know from Lemma 15 that $\mathrm{Ob}(v_1)$ is a set of points or arcs; and from Lemma 17 we know $\mathrm{Ob}(v_1)$ is a finite set of points, except for at most one t, at which it is a set of points and arcs. Thus if $v_1(t)$ avoids these obstructions, it avoids intersection with the remainder of the chain.

But now it should be clear that it is easy for $v_1(t)$ to "run away" from the obstructions. Think of its sphere of possible positions growing and shrinking with time t. $v_1(t)$ must avoid a set of points at any one time, and once (cf. Lemma 17), a set of arcs. This is easily done: there is no way to "cage" in $v_1(t)$ with these obstacles. Another view of this situation is that the configuration space $\mathbb{S}^2 \times \mathbb{R}_{[0,1)}$ is 3-dimensional, and the obstructions $\mathrm{Ob}(v_1(t))$ for $t \in [0, 1)$ are 1- or 0-dimensional, and the removal of a 1D set cannot disconnect a 3D set (cf. proof of Lemma 6).

The remainder of this subsection establishes this claim more formally. A *path* in a topological space X is a continuous function $\gamma : [0, 1] \to X$. A space is *path-connected* if any two of its points can be joined by a path [2]. We first work with the space $\mathcal{C}'_1$: the positions for v_1, for $t \in [0, 1)$. Later we will add in $t = 1$, and positions for v_3.

Lemma 18. *The free space $\mathcal{F}'_1 \subset \mathcal{C}'_1$ for v_1 in the configuration space $\mathcal{C}'_1 = \mathbb{S}^2 \times \mathbb{R}_{[0,1)}$ is path-connected.*

Proof. It will help to view our configuration space as follows. The 2-sphere S_1 is represented by a flat two-dimensional sheet, and $\mathbb{R}_{[0,1)}$ is represented as a vertical axis. The result is a three-dimensional space, analogous to Fig. 13, that could look as depicted in Fig. 15. The point obstacles $\mathrm{Ob}(v_1)$ become paths monotone with respect to the vertical t-axis. At one $t = t_1$ we may have arc obstacles as well. We need to show that $v_1(0)$ is connected by a path to $v_1(t')$, for any $t' < 1$. We proceed in two cases:

1. $\mathrm{Ob}(v_1)$ contains only points for all $t \in [0, 1)$. Let N be the maximum number of points in $\mathrm{Ob}(v_1)$ over all t; we know $N \leqslant 2n$. A 2-sphere with a finite number N points removed is path-connected. For each t, remove N points from the corresponding $S_1(t)$: those in $\mathrm{Ob}(v_1)$ at that t, and extra distinct points to "pad out" to N. Any two spheres with the same number of points removed are homeomorphic.
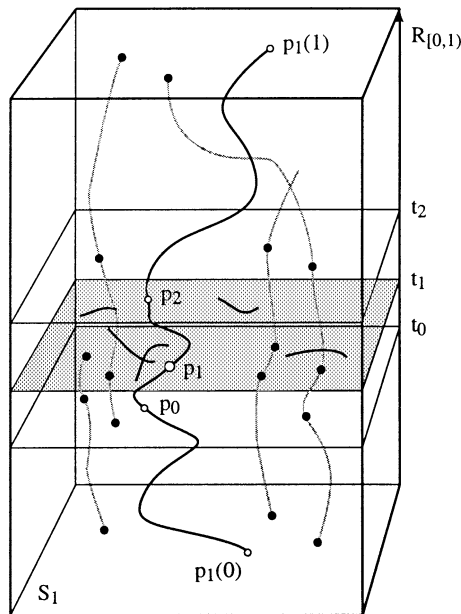
Fig. 15. The free space $\mathcal{F}_1$ for v_1 is path-connected. π_1 (dark) connects $p_1(0)$ to $p_1(1)$. $Ob(v_1)$ includes points at a fixed t, forming curves (shaded) over time. The shaded subspace at time $t = t_1$ includes arcs in $Ob(v_1)$.

Therefore $\mathcal{F}_1'$ is homeomorphic to $S_1(0) \times \mathbb{R}_{[0,1)}$. Because each of those spaces is path-connected, and the product of two path-connected spaces is path-connected, we have established the claim.

2. $Ob(v_1)$ contains arcs at $t = t_1$. The main idea here is to choose a point $p_1 = v_1(t_1)$ that is unobstructed at time $t = t_1$, and then connect from $v_1(0)$ to p_1, and from p_1 to $v_1(t')$. It is clear, as we have shown in Case 1, that the spaces $\mathcal{F}_- = \mathcal{C}_{/t \in [0,t_1)}$ and $\mathcal{F}_+ = \mathcal{F}_{/t \in (t_1, 1)}$ are path connected. We will prove that there exist points $p_0 \in \mathcal{F}_-$ and $p_2 \in \mathcal{F}_+$ such that p_0 and p_2 are connected by a path.

We will call a point p *free* if it does not belong to any obstruction diagram. Let $p_1 \in S_1(t_1)$ be a free point on S_1 at t. It is clear that such a point exists, since the obstruction diagram is a finite set of arcs and points. It is also clear that there exists a neighborhood $U \subset \mathcal{F}_1'$ of p_1 all of whose points are free. Choose $p_0 \in U$, $p_0 \in S_1(t_0)$, $t_0 < t_1$ and $p_2 \in U$, $p_2 \in S_1(t_2)$, $t_1 < t_2$. See Fig. 15. Both points are free and can be connected by a path in U to p_1. But $p_0 \in \mathcal{F}_-$ and $p_2 \in \mathcal{F}_+$, both path connected spaces. Thus we may connect $v_1(0)$ to p_0 to p_1 to p_2 to $v_1(t')$. $\square$

We now address the endpoint $t = 1$, extending C_1' to C_1 for $t \in [0, 1]$. As v_2 approaches q on L, one of the spheres, that for v_1 by our assumptions, shrinks to zero radius. Thus Fig. 15 is not an accurate depiction near $t = 1$, for the configuration space narrows to a point here.

Lemma 19. *The free space $\mathcal{F}_1$ for v_1 in the full configuration space $\mathcal{C}_1$ is path-connected.*

Proof. We have chosen q and L in Lemma 12 so that the $t = 1$ endpoint is free in the sense that the straightened chain $v_0 v_1 v_2$ does not intersect the fixed portion of the chain. Thus there is a neighborhood

U of $t = 1$ such that $\mathcal{C}_1$ is devoid of all obstructions within that neighborhood. Choose $t' \in U$ and apply Lemma 18 to yield a path from $v_1(0)$ to $v_1(t')$. Connect within U from $v_1(t')$ to the endpoint $v_1(1)$. $\quad\square$

Now we include v_3 in the analysis.

Lemma 20. *The free space $\mathcal{F} \subset \mathcal{C}$ for both v_1 and v_3 in the configuration space $\mathcal{C}$ for $t \in [0, 1]$ is path-connected.*

Proof. The key here is the independence of the motions of v_1 and v_3. Let π_1 be a path for $v_1(t)$ through $\mathcal{F}_1$, whose existence is guaranteed by Lemmas 18 and 19. Now construct $\mathcal{F}_3$ as the possible positions $v_3(t)$ for v_3, avoiding at each time $\text{Ob}(v_3(t))$, where this time the obstructions include not only the fixed links $s_4, s_5, \ldots, s_n$, but also the two moving links s_0 and s_1, determined by π_1. If $v_3(t)$ avoids $\text{Ob}(v_3(t))$ for each t, then all intersections are avoided: we do not need to include the moving links in $\mathcal{F}_1$, because intersection is symmetric—if the links s_2 and s_3 do not intersect s_0 and s_1, then s_0 and s_1 do not intersect s_2 and s_3.

For a fixed t, the obstacles are fixed segments, and $\text{Ob}(v_3)$ is again a finite set of points, or, for at most one t, a set of arcs: Lemmas 15 and 17 apply unchanged. The independence of the motion of v_3 from v_1 permits us to treat the moving segments s_0 and s_1 on par with the fixed segments: the only difference is that their obstacle points move through $\mathcal{C}_3$ differently. Therefore a path π_3 for $v_3(t)$ may be found in $\mathcal{F}_3 \subset \mathcal{C}_3$. The two paths π_1 and π_3, together with the ray L for v_2, constitute a path for moving the 4-link chain $(v_0, v_1, v_2, v_3, v_4)$ through $\mathcal{C}$ while maintaining simplicity. $\quad\square$

This finally completes the proof of Theorem 6.

4.4. Motion planning

We now know a path that avoids self-intersection exists, i.e., either the joint v_1 or v_3 can be straightened. The next step is to compute such a path algorithmically. We rely on general motion planning algorithms, as in Section 2.1.3.

Our "robot" consists of the four links $(v_0, v_1, v_2, v_3, v_4)$ moving in the 5-dimensional configuration space $\mathcal{C}$, Eq. (9). The subspace $\mathcal{C}_0$ that avoids self-intersection between the four links is some semialgebraic subset of $\mathcal{C}$, semialgebraic because the constraints on self-intersection may be written in Tarski sentences (see, e.g., [15]). The free configuration space $\mathcal{F}$ is composed of the points of $\mathcal{C}_0$ that avoid the obstacles, which is again a semialgebraic set. Canny's Roadmap algorithm achieves a time and space complexity of $O(n^5 \log n)$, where n is the number of obstacles, because in our case, the configuration space has $k = 5$ dimensions. The algorithm produces a piecewise algebraic path through $\mathcal{F}$, of $O(n^5)$ pieces. Each piece constitutes a constant number of moves, and so each joint straightening can be accomplished in $O(n^5)$ moves. Repeating the planning and straightening n times leads to $O(n^6)$ moves in $O(n^6 \log n)$ time. Because choosing L times requires at most $O(n^4)$ time by Lemma 12, the time complexity is dominated by the path planning, thereby establishing the bounds claimed in Theorem 3.

In the same way that Algorithm 1b improved on Algorithm 1a by avoiding motion planning, it is likely Algorithm 3 could be improved by an ad hoc algorithm.

5. Higher dimensions

We have already shown that every simple open chain or tree in 4D can be straightened, and every closed chain convexified. Our final task is to prove that these results hold for higher dimensions, using the results from 4D.

For an open chain, we straighten four links at a time and then repeat the procedure until the chain is straight. If the chain or tree contains fewer than four links, then it spans at most a k-flat for $k \leqslant 3$, and it can be included in $\mathbb{R}^4$. For a closed chain, our algorithm also moves four links at a time. Four links determine at most a k-flat H for $k \leqslant 4$ which means that it can be included in a 4-flat in $\mathbb{R}^d$, $d \geqslant 4$.

We have already shown that these four links, for both all types of chains, can be straightened in 4D; therefore, they can be straightened in this 4-flat $H \subset \mathbb{R}^d$. We only have to worry about the pieces of the remainder of the chain that intersect H. But since we are dealing with segments, their intersection with H is either a point or a segment. But these are the kind of obstructions we have proven that can be avoided in $\mathbb{R}^4$. Therefore, the straightening of these four links can be completed in H, and therefore in $\mathbb{R}^d$, while maintaining rigidity and simplicity.

The complexity for the algorithms in $\mathbb{R}^d$, $d \geqslant 4$, is the same as for the algorithms in 4D, for all computations are performed in 4-flats. This proves Theorem 4.

Acknowledgements

References

[1] C.C. Adams, The Knot Book, W.H. Freeman, New York, 1994.

[2] M.A. Armstrong, Basic Topology, McGraw-Hill, London, 1979.

[3] T. Biedl, E. Demaine, M. Demaine, S. Lazard, A. Lubiw, J. O'Rourke, M. Overmars, S. Robbins, I. Streinu, G.T. Toussaint, S. Whitesides, Locked and unlocked polygonal chains in 3D, in: Proc. 10th ACM-SIAM Sympos. Discrete Algorithms, January 1999, pp. 866–867; Full version: LANL arXive cs.CG/9910009.

[4] T. Biedl, E. Demaine, M. Demaine, A. Lubiw, J. O'Rourke, M. Overmars, S. Robbins, I. Streinu, G.T. Toussaint, S. Whitesides, On reconfiguring tree linkages: Trees can lock, in: Proc. 10th Canadian Conf. Comput. Geom., 1998, pp. 4–5; Full version: LANL arXive cs.CG/9910024, to appear in Discrete Math.

[5] J. Cantarella, H. Johnston, Nontrivial embeddings of polygonal intervals and unknots in 3-space, J. Knot Theory Ramifications 7 (8) (1998) 1027–1039.

[6] R. Cocan, Polygonal chains cannot lock in 4D, Undergraduate Thesis, Smith College, 1999.

[7] R. Cocan, J. O'Rourke, Polygonal chains cannot lock in 4D, in: Proc. 11th Canadian Conf. Comput. Geom., 1999, pp. 5–8.

[8] R. Connelly, E.D. Demaine, G. Rote, Straightening polygonal arcs and convexifying polygonal cycles, in: Proc. 41st Annu. IEEE Sympos. Found. Comput. Sci., IEEE, November 2000, pp. 432–442.

[9] R.H. Crowell, R.H. Fox, Introduction to Knot Theory, Blaisdell Publishing Co., New York, NY, 1965.

[10] H. Edelsbrunner, L.J. Guibas, J. Pach, R. Pollack, R. Seidel, M. Sharir, Arrangements of curves in the plane: Topology, combinatorics, and algorithms, Theoret. Comput. Sci. 92 (1992) 319–336.

[11] H. Edelsbrunner, R. Seidel, M. Sharir, On the zone theorem for hyperplane arrangements, SIAM J. Comput. 22 (2) (1993) 418–429.

[12] D. Halperin, Arrangements, in: J.E. Goodman, J. O'Rourke (Eds.), Handbook of Discrete and Computational Geometry, CRC Press, Boca Raton, FL, 1997, Chapter 21, pp. 389–412.

[13] J.G. Hocking, G.S. Young, Topology, Addison-Wesley, Reading, MA, 1961.

[14] W.J. Lenhart, S.H. Whitesides, Reconfiguring closed polygonal chains in Euclidean d-space, Discrete Comput. Geom. 13 (1995) 123–140.

[15] B. Mishra, Computational real algebraic geometry, in: J.E. Goodman, J. O'Rourke (Eds.), Handbook of Discrete and Computational Geometry, CRC Press, Boca Raton, FL, 1997, Chapter 29, pp. 537–558.

[16] G.T. Sallee, Stretching chords of space curves, Geometriae Dedicata 2 (1973) 311–315.

[17] P. Samuel, Projective Geometry, Springer, New York, 1988.

[18] M. Sharir, Algorithmic motion planning, in: J.E. Goodman, J. O'Rourke (Eds.), Handbook of Discrete and Computational Geometry, CRC Press, Boca Raton, FL, 1997, Chapter 40, pp. 733–754.